

## RESEARCH ARTICLE

# Quantitative systems pharmacology-based exploration of relevant anti-amyloid therapy challenges in clinical practice

Hugo Geerts<sup>1</sup>  | Silke Bergeler<sup>2</sup> | Mike Walker<sup>3</sup> | Rachel H. Rose<sup>4</sup> | Piet H. van der Graaf<sup>4</sup>

<sup>1</sup>Certara Predictive Technologies, Berwyn, Pennsylvania, USA

<sup>2</sup>BMS, Lawrenceville, New Jersey, USA

<sup>3</sup>Exscientia, Oxford, UK

<sup>4</sup>Certara Predictive Technologies, Sheffield, UK

## Correspondence

Hugo Geerts, Certara, 686 Westwind Dr, Berwyn, PA 19312, USA.

Email: [hugo.geerts@certara.com](mailto:hugo.geerts@certara.com)

## Abstract

**INTRODUCTION:** Addressing practical challenges in clinical practice after the recent approvals of amyloid antibodies in Alzheimer's disease (AD) will benefit more patients. However, generating these answers using clinical trials or real-world evidence is not practical, nor feasible.

**METHODS:** Here we use a Quantitative Systems Pharmacology (QSP) computational model of amyloid aggregation dynamics, well validated with clinical data on biomarkers and amyloid-related imaging abnormality–edema (ARIA-E) liability of six amyloid antibodies in clinical trials to explore various clinical practice challenges.

**RESULTS:** Treatment duration to reach amyloid negativity ranges from 12 to 44, 16 to 40, and 6 to 20 months for lecanemab, aducanumab, and donanemab, respectively, for baseline central amyloid values between 50 and 200 Centiloids (CL). Changes in plasma cerebrospinal fluid A $\beta$ 42 and the plasma A $\beta$ 42/ A $\beta$ 40 ratio—fluid biomarkers to detect central amyloid negativity—is greater for lecanemab than for aducanumab and donanemab, indicating that these fluid amyloid biomarkers are only suitable for lecanemab. After reaching amyloid negativity an optimal maintenance schedule consists of a 24-month, 48-month and 64-month interval for 10 mg/kg (mpk) lecanemab, 10 mpk aducanumab, and 20 mpk donanemab, respectively, to keep central amyloid negative for 10 years. Cumulative ARIA-E liability could be reduced to almost half by introducing a drug holiday in the first months. For patients experiencing ARIA-E, restarting treatment with a conservative titration strategy resulted in an additional delay ranging between 3 and 4 months (donanemab), 5 months (lecanemab), and up to 7 months (aducanumab) for reaching amyloid negativity, depending upon the timing of the incident. Clinical trial designs for Down syndrome patients suggested the same rank order for central amyloid reduction, but higher ARIA-E liability especially for donanemab, which can be significantly mitigated by adopting a longer titration period.

**DISCUSSION:** This QSP platform could support clinical practice challenges to optimize real-world treatment paradigms for new and existing amyloid drugs.

This is an open access article under the terms of the [Creative Commons Attribution-NonCommercial](https://creativecommons.org/licenses/by-nc/4.0/) License, which permits use, distribution and reproduction in any medium, provided the original work is properly cited and is not used for commercial purposes.

© 2024 The Authors. *Alzheimer's & Dementia: Translational Research & Clinical Interventions* published by Wiley Periodicals LLC on behalf of Alzheimer's Association.

## 1 | INTRODUCTION

The approval of new amyloid antibodies has raised new challenges with regard to the treatment of Alzheimer's disease (AD) patient populations in clinical practice that share few communalities with the populations selected for the clinical trials. To document the performance of the different antibodies in clinical practice, new initiatives have been proposed. Validating fluid biomarkers as markers of treatment effect can significantly increase uptake in the AD clinical practice.<sup>1</sup> ALZ-NET,<sup>2</sup> supported by the Alzheimer's Association, is a repository for documenting efficacy and side effects of patients on amyloid antibody therapies. Over time this will yield valuable information on the profile of responders and the factors that are associated with increased liability for amyloid-related imaging abnormality–edema (ARIA-E) side effects and ultimately optimize treatment guidelines.

In the meantime, we can propose best treatment guidelines based on extensive analysis of the limited number of subjects in the clinical trials with both positive and negative outcomes. Current published treatment guidelines<sup>3,4</sup> are available for selecting patients and doses, and providing strategies to mitigate side effects. However, a number of questions remain. For instance, how would resuming treatment after an ARIA-E incidence affect amyloid biomarker response, how to define the time of reaching amyloid negativity using easily accessible fluid biomarkers rather than imaging biomarkers, how to define a maintenance dose once this threshold is achieved, and finally, can we devise new strategies to mitigate ARIA-E liability?

Attempts towards achieving these goals are underway based on the large datasets available from clinical trials, and recently practical management strategies of ARIA-E have been proposed based on experience with patients on aducanumab.<sup>5</sup> However, there is room for a more comprehensive understanding of these therapies and management of their side effects.

A possible solution is to use a predictive Quantitative Systems Pharmacology (QSP) approach that describes the biomarker changes and ARIA-E liability at the group level from published clinical trials and applies the results to individual patient situations. This mechanistic QSP model<sup>6</sup> is based on detailed biological and biophysical insights about the aggregation and clearance processes of amyloid beta ( $A\beta$ ) species and is therefore generalizable beyond the clinical trials and the antibodies used for model calibration. The model outcome in terms of amyloid imaging and fluid biomarkers as well as ARIA-E liability is fully calibrated using clinical data on longitudinal observational studies as well as interventional studies with the six antibodies bapineuzumab, solanezumab, crenezumab, gantenerumab, aducanumab, and lecanemab. To illustrate the generalizability of the platform, we first used the QSP model to simulate the amyloid biomarker readouts and ARIA-E liability of donanemab from the TRAILBLAZER<sup>7</sup> and gantenerumab from the Graduate I and II Phase 3 studies,<sup>8</sup> data that were not used in the model calibration, and compared these with the clinical observations.

A first question in clinical practice is determining the duration of treatment for aducanumab, lecanemab, and donanemab to reach

### RESEARCH IN CONTEXT

- Amyloid antibodies are new therapeutic modalities in Alzheimer care, but patient populations in clinical trials are different from the real-world population in clinical practice.
- An advanced computer simulation model, previously validated using clinical trial data from six antibodies, allows optimizing clinical biomarker readouts for real-world patient conditions for each of the individual antibodies.
- The model identifies treatment durations for reaching amyloid negativity and optimal maintenance dosing to avoid rebounding of amyloid in addition to relevant fluid biomarker changes that can be monitored instead of positron emission tomography imaging.
- The model suggests optimal titration scenarios for restarting treatment after amyloid-related imaging abnormality–edema (ARIA-E) incidence.
- The model identifies timing of drug holidays to mitigate ARIA-E risk.
- A clinical trial design is proposed for Down syndrome patients.

amyloid negativity, as dosing can then be switched to a maintenance treatment schedule. The gold standard is amyloid positron emission tomography (PET) imaging to achieve an amyloid load of 25 centiloids (CL) or less.<sup>9</sup> However, this is expensive and not easily accessible, leading to the need to define peripheral biomarkers, especially plasma, for determining the optimal treatment duration.

We therefore investigated the influence of the approved medications on the dynamics of cerebrospinal fluid (CSF)  $A\beta_{42}$  and plasma  $A\beta_{42}/A\beta_{40}$  in relation to changes in central amyloid load to explore which peripheral biomarker could be a reliable biomarker for reaching amyloid negativity. Although standardized uptake value ratio (SUVR) amyloid is the biomarker of choice, we also simulated the effect of the antibodies on the changes in protofibrils, as these have been suggested to drive additional neurotoxicity.<sup>10</sup> We subsequently explored various maintenance dosing schedules in order to keep amyloid load below threshold for a long follow-up period.

A second important challenge is restarting treatment after interruption due to an ARIA-E incident. We explored new scenarios to optimize the benefit-risk ratio for each individual antibody.

In order to address how variability in a clinical trial setting alters outcomes across these amyloid antibody treatments, we simulated the biomarker trajectory of a virtual patient population of 200 subjects with sampling of the key parameters to compare the amyloid load biomarkers and ARIA-E liability of these antibody therapies on a patient-per-patient basis. These results illuminate the processes driving the fraction of amyloid responders and ARIA-E incidence and are a first step towards personalized medicine.

Finally, Down syndrome (DS) patients are an important but under-served part of the autosomal dominant AD spectrum. Here we use the QSP model to propose clinical trial designs with the three antibodies for this population.

## 2 | METHODS

### 2.1 | Amyloid biomarkers

The QSP model used for simulations of various scenarios on amyloid readouts has been published before.<sup>6</sup> Basically, the model consists of a physiologically-based pharmacokinetic (PBPK) model coupled to a mechanistic QSP model of amyloid aggregation. The PBPK model<sup>11</sup> lumps peripheral tissues together but models explicitly lymph, plasma, four different CSF and the interstitial fluid (ISF) compartments including the blood-brain barrier (BBB) and the blood-CSF-barrier (BCSFB). Conversely, this platform can be used to derive the level of peripheral biomarkers such as monomeric A $\beta$ 40 and A $\beta$ 42 in lumbar CSF and plasma, both free and antibody-bound. The mechanistic QSP model describes the synthesis of A $\beta$  from the precursor protein amyloid precursor protein (APP), the enzymatic degradation of the monomer by insulin-degrading enzyme (IDE) or neprilysin, the aggregation of monomers into oligomers, protofibrils, and plaques, and the clearance of oligomers, protofibrils and plaques by microglia. We consider monomers ( $n = 1$ ), oligomers ( $n = 2-16$ ) with molecular weights (MWs) between 8 and 80 kDa, protofibrils ( $n = 17-24$ )<sup>12</sup> with MW > 80 kDa and plaques ( $n = 25$ ). The apolipoprotein E  $\epsilon$ 4 allele (APOE4) genotype is introduced using a differential effect on A $\beta$  clearance by microglia.<sup>13</sup> Key observable readouts include SUVR amyloid, CSF A $\beta$ 40 and A $\beta$ 42, and plasma A $\beta$ 42/A $\beta$ 40, which have been calibrated previously in both longitudinal and interventional clinical studies. Notably the levels of soluble oligomers and protofibrils and insoluble plaques were constrained from postmortem biochemical studies in AD brains. The following formula describes the calculation of SUVR amyloid, based on different contributions of soluble and insoluble A $\beta$  aggregates, with the four parameters fixed for optimal correlation with the clinical data:

$$SUVR_w = 1 + \frac{C_1 \left( Ab42^{oligo} + Ab42^{proto} + C_2 * Ab42^{plaque} \right)^{C_3}}{\left[ \left( Ab42^{oligo} + Ab42^{proto} + C_2 * Ab42^{plaque} \right)^{C_3} + C_4 C_3 \right]}$$

Furthermore, the SUVR amyloid for florbetapir can be calculated in CL using the formula Amyloid (CI) = 183\*SUVR-177.<sup>14</sup>

Modeling the binding between antibodies and plaques in a perivascular compartment with a time-to-event relationship has been demonstrated to predict the clinically observed ARIA-E rates.

The model takes PK and pharmacological (ie, affinities for the different A $\beta$  species) properties of the antibodies into account and can simulate various treatment scenarios, including titration schedules, protocol amendments, and treatment holidays. Because the aggregation dynamics are explicitly modeled in a biophysically realistic way, this allows derivation of the dynamics of fluid biomarkers from changes

in SUVR amyloid imaging as well as the optimal maintenance schedule once central amyloid negativity has been achieved. Using the perivascular compartment plaque bound antibody levels as the best readout for ARIA-E liability, the model allows exploration of the impact of restarting treatment using a specific titration schedule after an ARIA-E incident as well as the impact of a drug holiday on ARIA-E liability.

As both CSF and plasma A $\beta$  concentrations are an output of the platform, we can investigate the relationship between changes in these fluid biomarkers and central amyloid dynamics, possibly identifying thresholds in peripheral biomarkers that would indicate reaching amyloid negativity.

### 2.2 | Virtual trial

Biological processes that can be unique for individual patients include synthesis and degradation of A $\beta$  monomers, forward and backward rate constants of primary nucleation for higher-order aggregates, enhanced forward aggregation due to secondary nucleation, breakdown of protofibrils into smaller aggregates, and uptake of various A $\beta$  species by microglia cells. Additionally, there are treatment-associated processes such as variability of drug uptake at the BBB and the phenotypic switch from low to high phagocytosing phenotype after binding of the antibody to the Fc-gamma receptor (Fc $\gamma$ R) on microglia cells. We generated virtual patients by sampling parameters associated with these processes from a Gaussian distribution with a coefficient of variation (CV) of 10% to 30% depending upon the individual parameter (see [Supplementary Information](#) for more details).

For each of these patient and drug pharmacology profiles, a natural history trajectory was simulated. A reasonable technically feasible approach was to define the onset of AD pathology when the CSF A $\beta$ 42 concentration dropped below 0.17 nM.<sup>15</sup> However, because the CSF A $\beta$ 42 cutoff values tend to underestimate central amyloid SUVR amyloid cutoff values<sup>16</sup> and clinical trials were focused on amyloid-positive subjects, we therefore identified the age at which the SUVR amyloid exceeded 1.30 or 47 CL (Age\*) and delayed the start of the trial with the following relationship, assuming an average delay of 6 years between diagnosis and treatment start.

$$\text{Start\_Trial} = \text{Age}^* + 2 + 8 * \text{RND}[0, 1]$$

where the random function (RND) is sampled from a uniform distribution between 0 and 1. In this way a baseline amyloid load with most patients in the range 80 to 120 CL is achieved.

### 2.3 | Simulation of amyloid dynamics in Down patients

The QSP model is applied to the specific pathology in autosomal dominant AD patients with DS by assuming a 50% higher synthesis of the APP, leading to a higher influx of monomeric A $\beta$ 40 and A $\beta$ 42 into the brain parenchyma. This is based upon the observations that central DS

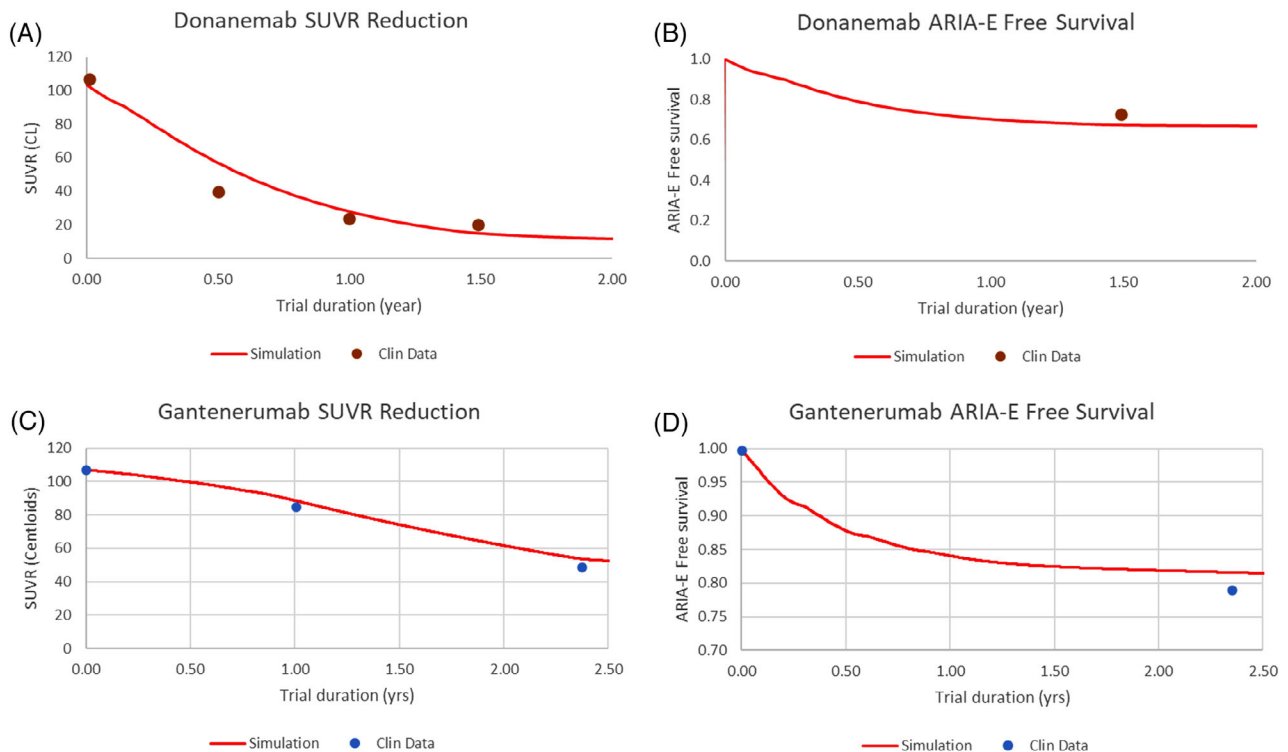


**FIGURE 1** When introducing the pharmacology and PK profile of donanemab and gantenerumab, the model reproduces the biomarker dynamics observed in donanemab's TRAILBLAZER trials (A,B) and gantenerumab's GRADUATE trials (C,D), both for central amyloid readouts (A,C) and ARIA-E liability (B,D). Circles are clinically reported data (Clin Data). Data were compared to placebo. ARIA-E, amyloid-related imaging abnormality–edema; CL, centiloids; SUVR, standardized uptake value ratio.

phenotype is associated with the specific triplication of APP on chromosome 21.<sup>17</sup> Implementing these changes leads to a steep decrease in CSF A $\beta$ 42 and a steep increase in SUVR amyloid at about 10–15 years earlier than in AD patients.

### 3 | RESULTS

#### 3.1 | Predicting amyloid load and ARIA-E side effect for new antibody

As mentioned before, the model has been calibrated on group average data solanezumab, crenezumab, bapineuzumab, gantenerumab, aducanumab, and lecanemab. To demonstrate its generalizability, we simulated the biomarker effect of donanemab, an antibody against the pE3 epitope present in amyloid plaques, from the Phase 2 TRAILBLAZER study, starting at 10 mg/kg (mpk) for the first 3 months followed by 15 months of 20 mpk. The plasma PK profile was fitted from reported data<sup>18,19</sup> and the dissociation constant  $K_d$  was derived from experimental data<sup>20</sup> to be 0.14 nM for plaques and a much smaller affinity ( $K_d = 50$  nM) for soluble A $\beta$  aggregates. Figure 1A,B shows that the model reasonably well reproduces both the observed changes in PET SUVR amyloid and the time-dependent incidence of ARIA-E.

Similarly, we investigated the amyloid dynamics and ARIA-E liability of gantenerumab using the GRADUATE Phase 3 study design. This trial did not meet the primary endpoints,<sup>8</sup> likely because of a smaller than

expected decline in SUVR amyloid. Using the specific titration schedule of these studies, the model was able to reproduce both the amyloid dynamics and ARIA-E liability (Figure 1C,D). Because the model takes into account the complex interaction of the antibody with the different A $\beta$  species in addition to their aggregation dynamics and the microglia biology, these mechanism-driven predictions could be somewhat different from data-driven PKPD analysis, especially if different dose-intervals are considered. In general, leveraging this QSP model in the future could set the standard for early development of future amyloid neurotherapies for AD, especially in cases with limited clinical data.

#### 3.2 | Achieving amyloid negativity

Although ARIA-E risk diminishes over time,<sup>21</sup> it is suggested to limit exposure to amyloid-removing antibodies in patients once amyloid negativity is achieved. In this section we provide estimates of the minimum treatment duration for individual antibodies (aducanumab, lecanemab, donanemab, and gantenerumab) to achieve amyloid negativity as a function of the patient's baseline amyloid load at the start of treatment. Amyloid negativity is defined as reaching a threshold of 25 CL as assessed with florbetapir imaging.<sup>16</sup>

These dosing schedules are 1 mpk Q4W for 3 months, 3 mpk Q4W for 3 months, 6 mpk Q4W for 3 months, followed by 10 mpk Q4W for aducanumab; 10 mpk Q2W for lecanemab during the whole treat-

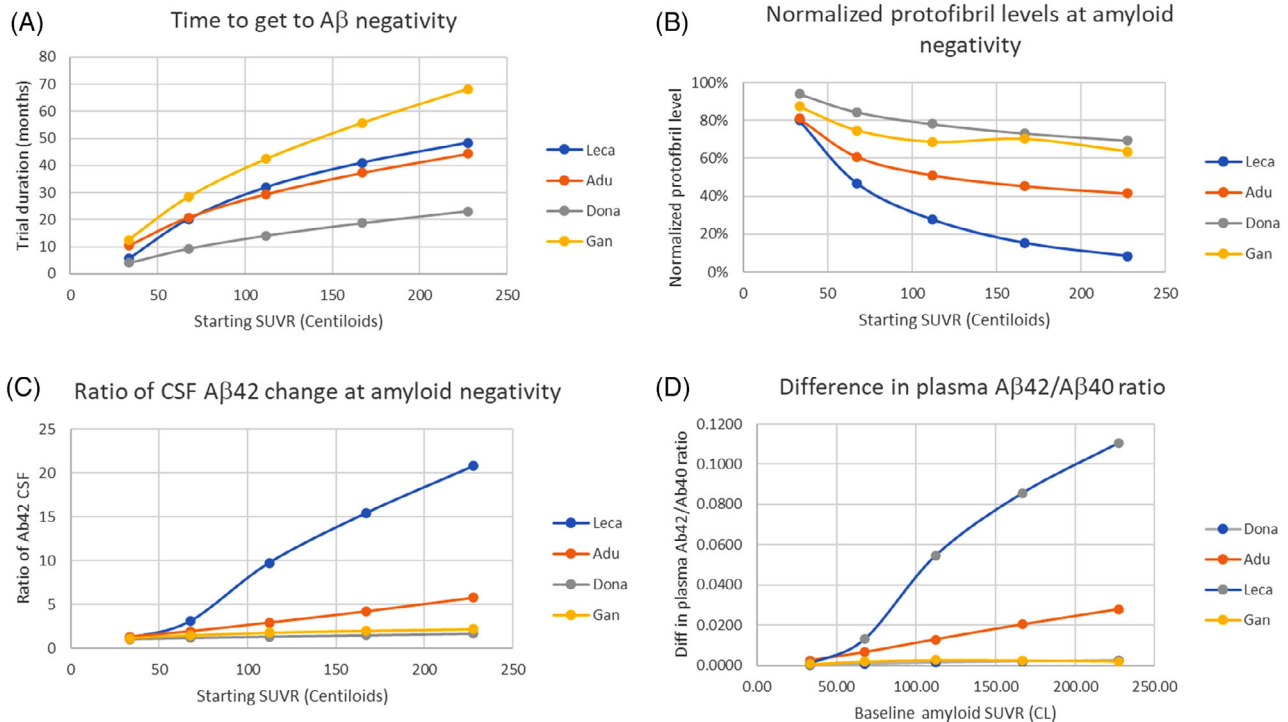


**FIGURE 2** Outcomes simulated for donanemab, lecanemab, aducanumab, and gantenerumab to reach amyloid negativity for a range of baseline central amyloid values using the reported titration schedules from the Phase 3 studies. All outcomes are for an APOE4+ subject. (A) Duration to reach amyloid negativity ranges from 4 to 23 months for donanemab, 5 to 48 months for lecanemab, 10 to 44 months for aducanumab, and 10 to 70 months for gantenerumab. (B) Final protofibril levels normalized to baseline at time of reaching amyloid negativity. Lecanemab has the greatest reduction, followed by aducanumab, gantenerumab, and donanemab. (C) Increase in CSF A $\beta$ 42 normalized against baseline at the time of reaching amyloid negativity as a function of baseline amyloid load is greatest for lecanemab, followed by aducanumab, and much smaller for donanemab and gantenerumab. (D) Difference from baseline in plasma A $\beta$ 42/A $\beta$ 40 ratio at the time of reaching amyloid negativity for different baseline amyloid central amyloid levels. The difference is greatest for lecanemab. A $\beta$ , amyloid beta; Adu, aducanumab; APOE4, apolipoprotein E  $\epsilon$ 4 allele; CL, centiloids; CSF, cerebrospinal fluid; Dona, donanemab; Gan, gantenerumab; Leca, lecanemab; SUVR, standardized uptake value ratio.

ment; 10 mpk Q4W for 3 months, followed by 20 mpk Q4W for donanemab (all iv infusions). For gantenerumab, we simulated 120 mg Q4W, 255 mg Q4W, and 510 mg Q4W followed by 510 mg Q2W (all subcutaneous). Figure 2A shows predicted times to reach amyloid negativity treatment with different antibodies starting from different baseline values, where we allowed the treatment to continue beyond 18 months. As expected, for the dosing schedules described above and all baseline amyloid loads, amyloid negativity (defined as less than 25 CL) is achieved faster for donanemab, as compared to lecanemab and aducanumab, while gantenerumab takes much longer. For baseline amyloid loads between 40 and 185 CL, treatment durations range between 3.7 and 25 months for donanemab, 6 and 50 months for lecanemab, between 10 and 47 months for aducanumab, and between 12 and 70 months for gantenerumab.

The gold standard for detecting amyloid negativity is a PET-scan based SUVR amyloid readout; however, this is expensive and not easily accessible. An alternative approach is to measure fluid biomarkers, such as CSF A $\beta$ 42 and plasma A $\beta$ 42/A $\beta$ 40. Previously we have demonstrated the relationship between changes in these fluid biomarkers and central amyloid load in observational natural history studies.<sup>6</sup> We next investigated changes in these easily accessible fluid biomarkers pre- and posttreatment with amyloid antibodies.

Secondary readouts in clinical trials have indeed demonstrated an increase in CSF A $\beta$ 42 and the plasma A $\beta$ 42/A $\beta$ 40 ratio to varying degrees following treatment. This is likely due to the clearance of higher-order aggregates that leads to a reduction of the secondary nucleation pathway and is dependent upon the specific pharmacology and titration schedule of the antibodies making a one-size-fits-all criterion challenging. Figure 2 demonstrates that the relation between increases in CSF A $\beta$ 42 (Figure 2C) and plasma A $\beta$ 42/A $\beta$ 40 (Figure 2D) at the time of reaching amyloid negativity is dependent upon the nature of the antibody with lecanemab showing the greatest dynamic range, followed by donanemab, aducanumab, and gantenerumab. This underscores the need for an antibody-specific criterion when using fluid biomarkers as a marker for amyloid negativity.

Finally, to illustrate the capacity of the model to predict the dynamics of intermediate and non-accessible A $\beta$  species, we simulated the reduction of protofibrils for the different antibodies at the time of reaching amyloid negativity. The level of soluble protofibrils has been suggested to drive neurotoxicity at least for in vitro systems,<sup>10,22,23</sup> although the clinical significance remains unclear. Figure 2B demonstrates that lecanemab has indeed the biggest effect in reducing protofibrils levels, reducing protofibrils by 70% to 90% for baseline amyloid level over 120 CL. Note that donanemab is only able to reduce



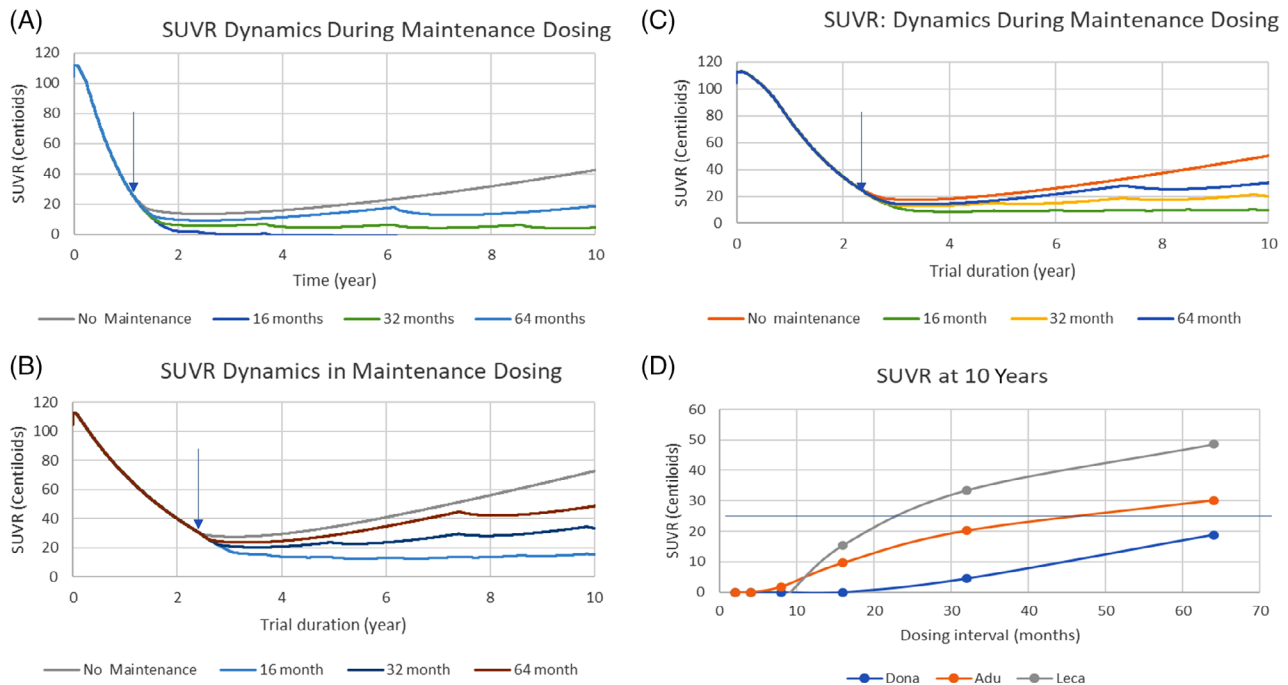


**FIGURE 3** SUVR AMYLOID dynamics in maintenance treatment for a 75-year-old APOE4+ subject after reaching amyloid negativity and switching to increasing intervals (in months) at the last dose for (A) donanemab, (B) lecanemab, and (C) aducanumab. (D) Central amyloid levels attained 10 years after regular treatment until amyloid negativity, followed by maintenance treatment at different intervals for the different antibodies. Time at which dosing is switched to maintenance is indicated with the arrow. In order to keep amyloid levels below the positivity threshold (25 CL) for this period, aducanumab and donanemab can be given every 48 and >60 months respectively, while lecanemab needs to be applied every 24 months. Adu, aducanumab; CL, centiloids; Dona, donanemab; Leca, lecanemab; SUVR, standardized uptake value ratio.

these levels by 20% to 30%, because of the much shorter duration to achieve amyloid negativity.

### 3.3 | Maintenance dosing

Once amyloid negativity has been reached, treatment can be switched to a maintenance schedule during which the slow rebound of amyloid plaques needs to be mitigated. The most convenient way for patients is to continue treatment with the last dose but increase the dosing interval.

As monomers and oligomers can bind to plaques in the aggregation process (secondary nucleation), the rate at which SUVR amyloid rebounds is dependent upon the relative level of amyloid plaques and intermediate A $\beta$  species at treatment halt. This might be dependent upon the pharmacology of the individual antibody.

Simulation data suggest that after treatment halt when amyloid negativity is reached, in the absence of any drug, amyloid load increases by about 4.1 to 5.8 CL/year depending upon the amyloid level after treatment (see Figure S5). We simulated the amyloid dynamics for a fixed baseline of 110 CL, and upon reaching a central amyloid level of 25 CL, switched to the same dose but with increasing intervals and generated amyloid profiles out for 10 years to mimic these levels seen in the patient population. Figure 3 shows the dynamics of central amyloid levels after treatment halt for donanemab (Figure 3A), lecanemab (Figure 3B) and aducanumab (Figure 3C), continuing at the same dose

but with increasing dosing intervals. The switch to maintenance treatment is initiated at 12, 30, and 32 months for donanemab, aducanumab, and lecanemab respectively. It is of interest to note that amyloid clearance continues for a certain time proportional to the half-life of the activated microglia phenotype. Figure 3D provides an overview of the central amyloid levels reached at 10 years when providing the antibodies at different intervals. To keep amyloid negativity at 10 years, the data suggest that interval ranges from longer than 64 months for donanemab at 20 mpk, to over 48 months for aducanumab at 10 mpk, but only 24 months for lecanemab 10 mpk. This is likely due to the latter's shorter half-life and higher affinity for protofibrils which leads to a lower reduction in amyloid plaque load.

We also simulated the dynamics of CSF A $\beta$ 42, the plasma A $\beta$ 42/A $\beta$ 40 ratio, and protofibrils during maintenance treatment (see Supplementary Information, Figures S1–3). In line with the observations over an 18-month trial, lecanemab achieves higher values of CSF A $\beta$ 42 and plasma A $\beta$ 42/A $\beta$ 40 and lower values of protofibrils at earlier time points. This difference is consistent across all time points and for any dosing interval.

### 3.4 | Treatment resumption after Aria-E incidence

We next studied the impact of treatment interruption for 12 weeks due to ARIA-E incidence, followed by a conservative titration schedule, on central amyloid biomarkers. After 3 months of interruption,

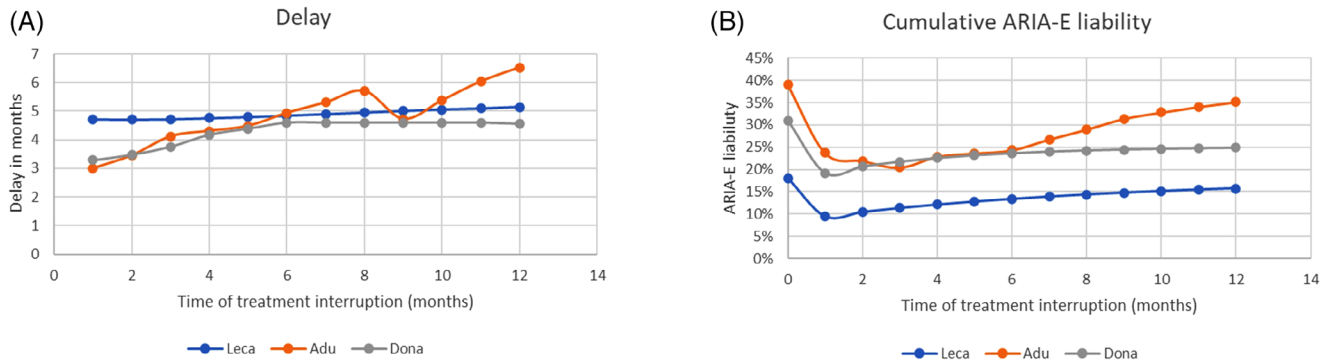


**FIGURE 4** (A) Additional delay for reaching amyloid negativity after interrupting treatment for 12 weeks after an ARIA-E incident at a specific time after treatment start. After the incident treatment is restarted using a conservative titration schedule of single 1 mpk, 3 mpk, 6 mpk (and 10 mpk for donanemab) doses Q4W before reaching the original dosing before the ARIA-E. The delay ranges from 3 to 7 months and is smallest for donanemab. While the delay for lecanemab (between 4 and 5 months) is independent of the timing, for both donanemab and aducanumab the delay increases as the incident happens later, likely due to interference with the titration schedule. (B). Introduction of a 3-month drug holiday in the titration schedule in the absence of ARIA-E at any time during the first 12 months can maximally reduce ARIA-E liability with 8% for lecanemab, 12% for donanemab, and 18% for aducanumab. ARIA-E at time  $t = 0$  months reflects the maximal liability using the titration schedules of the Phase 3 studies. The greatest impact is for an early drug holiday (first two months) for lecanemab and donanemab, while the window between 4 and 10 months is optimal for aducanumab. Adu, aducanumab; ARIA-E, amyloid-related imaging abnormality–edema; Dona, donanemab; Leca, lecanemab.

treatment restarted with 2 months of one-eighth of the maximal dose, 2 months of one-fourth the maximal dose, 2 months of one-half the maximal dose, followed by the maximal dose (maximal dose is 10 mpk Q2W for lecanemab, 10 mpk Q4W aducanumab, and 20 mpk Q4W for donanemab).

Depending upon the time at which the treatment is halted for ARIA-E, for a 75-year-old APOE4 patient, Figure 4A shows that the additional time delay (not including the drug holiday) to reach amyloid negativity ranges from 4.7 to 5.1 months for lecanemab, from 3.3 months to 4.6 months for donanemab, and from 3 to 7 months for aducanumab. Given the long duration of AD and the slow dynamics of  $A\beta$  aggregation, this delay is unlikely to be clinically significant.

Interestingly, even in situations without actual ARIA-E incidence, the simulations also suggest that having a drug holiday within the first months of treatment could reduce accumulated ARIA-E liability by 8% for lecanemab, 18% for aducanumab, and 12% for donanemab (Figure 4B), depending upon the timing of the drug holiday. A similar observation has been proposed using a different *in silico* model of ARIA-E.<sup>21</sup>

This happens without a big effect on biomarker dynamics (see Supplementary Information, Figure S4). In general, the model allows for a wide variety of titration schedules to be explored.

### 3.5 | Mitigating response variability

To get a better idea about the variability in clinical practice, we next simulated the effects of an 18-month treatment with donanemab, lecanemab, and aducanumab in the same virtual patient cohorts of 200 APOE4+ patients on biomarkers and ARIA-E liability. For this simulation, we assumed the same titration schedule as used in the pivotal Phase 3 studies and for the same duration (see Figure 5). This sim-

ulation provided us an estimation of a head-to-head comparison and helped to identify specific characteristics of responders for each of the individual antibodies. On average, donanemab has the fastest amyloid clearance, followed by lecanemab and aducanumab (Figure 5); however, this is associated with a much higher fraction of patients experiencing ARIA-E (31% for donanemab vs 18% for lecanemab). When calculating a therapeutic index (TI) as the ratio of decrease in amyloid levels (in CL and normalized to baseline amyloid) divided by the ARIA-E liability, lecanemab comes out on top, followed by aducanumab and donanemab. Interestingly in about 10% and 35% of cases, the TI is greatest in donanemab and aducanumab respectively. Because aducanumab has such a long titration schedule, it can mitigate ARIA-E liability at the expense of a substantial reduction in central amyloid. Balancing efficacy against ARIA-E side effects applies in general to any dosing strategy for amyloid antibodies.

Interestingly, these simulations suggest a linear relationship between final central amyloid after 18 months of treatment and the subsequent slope of central amyloid increase, such that the higher central amyloid at end of treatment, the faster the amyloid load in the patient rebounds to the baseline level (Figure S5). This suggests that plaques, due to their sheer number, indeed play a dominant role as mediators for secondary nucleation. Secondary nucleation is defined as the enhanced binding of an oligomer attached to the surface of the plaque, compared to binding of a monomer to an oligomer in solution. The more plaque surface is exposed, the more monomers are interacting with plaque-bound oligomers. The slope is greatest for lecanemab, because of the relative lower contribution of plaque degradation. The exact relationship depends upon the differential contributions and aggregation kinetics of the remaining  $A\beta$  species, each contributing to the calculation of the central amyloid biomarker. Larger virtual patient trials and a more detailed analysis of the intermediate  $A\beta$  species dynamics are needed to address this question.

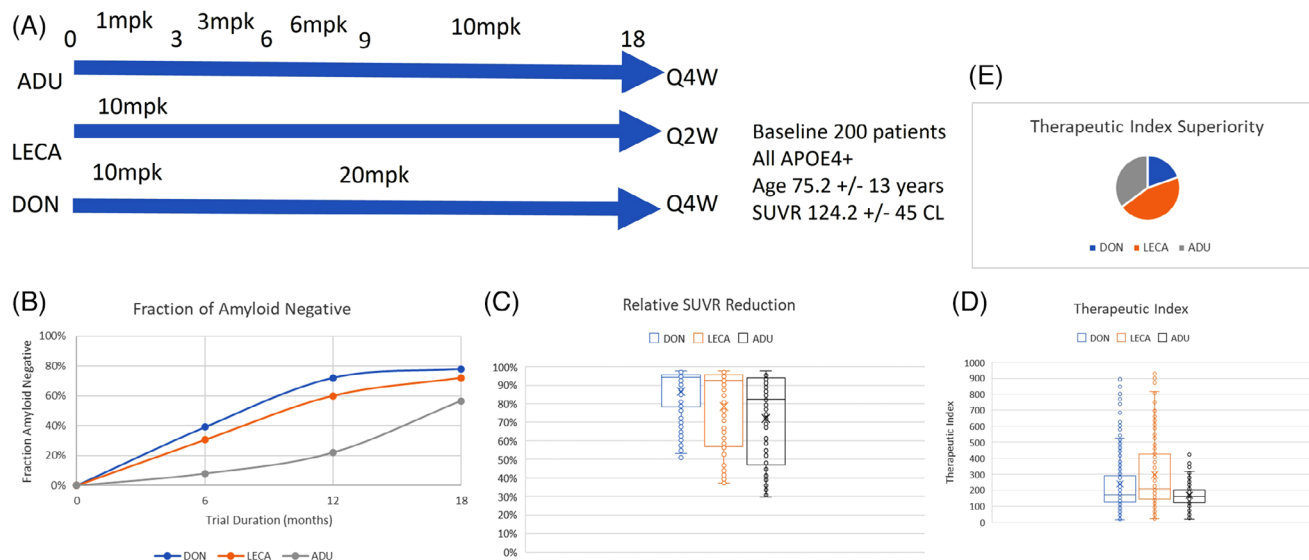


**FIGURE 5** Virtual patient trial of 200 APOE4+ subjects (50% female) with an average age of  $75 \pm 13$  years and a baseline central amyloid of  $124 \pm 45$  CL and each patient treated with the three different antibodies with their appropriate titration schedules. (A) Titration schedules for the three antibodies. (B) The fraction of amyloid negative patients at any time is greatest for donanemab, while aducanumab catches up with lecanemab only at 18 months. (C) Box-and whisker plots (median, upper and lower quartile) for central amyloid reduction showing the greatest effect for donanemab. (D) By defining a therapeutic index as fractional central amyloid reduction normalized to baseline divided by ARIA-E liability, lecanemab has on average the greatest impact compared to aducanumab and donanemab on the same patient population. (E) Diagram showing the fraction of patients for which the therapeutic index is the highest, demonstrating that the majority has the greatest benefit with lecanemab, although sizeable minorities have better outcome with aducanumab and donanemab. ADU, aducanumab; APOE4, apolipoprotein E  $\epsilon$ 4 allele; CL, centiloids; DONA, donanemab; LECA, lecanemab; mpk, mg/kg; SUVR, standardized uptake value ratio.

### 3.6 | Clinical trials in autosomal dominant AD DS patients

We finally simulated clinical trials in DS patients, an autosomal dominant Alzheimer disease population currently underserved but potentially responsive to amyloid antibodies. We used the titration schedules from their Phase 3 studies and for a duration of 18 months with the three antibodies according to their respective titration schedules. Simulation of the natural history reveals a decrease of CSF A $\beta$ 42, which is associated with the sudden increase in aggregation of monomeric central A $\beta$  peptides, about 15 years earlier than for AD patients. This is due to the continuous higher synthesis of monomeric A $\beta$ 40 and A $\beta$ 42 as a consequence of the trisomy 21.

Both amyloid biomarkers and ARIA-E liability were simulated for generic APOE4+ patients entering a clinical trial at 47, 50, and 52 years. Figure 6 shows that donanemab has the fastest clearance of central amyloid load (Figure 6A) and the highest ARIA-E liability (Figure 6B) for an average DS patient at the age of 47. When calculating a TI as the ratio of biomarker reduction divided by ARIA-E side effect liability, lecanemab is superior to donanemab and aducanumab, which holds for different ages of trial start (Figure 6D). In addition, the relative decrease of amyloid load for the three antibodies is smaller with increasing age (85% to 66% for donanemab, 49% to 30% for lecanemab, and 27% to 25% for aducanumab) because of the higher baseline amyloid load.

Interestingly, when simulating a more extensive titration schedule for donanemab, with doses starting at 2.5 mpk, followed by 5, 10, and

20 mpk, the ARIA-E side effect can be substantially lower in DS patients (Figure S6). In this case, the ARIA-E liability of 46% at the Alzheimer dosing schedule can be reduced to 37%, 26%, and 20% for a total duration of 3, 6, and 9 months up-titration, without much impact on central amyloid reduction (less than 5 CL).

## 4 | DISCUSSION

Using a clinically validated QSP model,<sup>6</sup> this paper explores a number of challenges in clinical practice for treatment with the two approved amyloid antibody medications, aducanumab and lecanemab, as well as donanemab—which has filed for approval. This biophysically realistic computer model combines aggregation dynamics and microglia-dependent clearance together with PBPK modeling of amyloid antibody target exposure and engagement with readouts for SUVR amyloid PET imaging and ARIA-E liability, both important drivers of clinical response. Each of these antibodies affects the different A $\beta$  species differently based on their affinity, with unique effects on the aggregation kinetics, resulting in different dynamics not only for amyloid-related biomarkers, but also for key intermediate species. The model captures very well the available biomarker dynamics for both the natural history as well as the effect of six different antibodies. The model can simulate the observed biomarker dynamics and ARIA-E liability for donanemab in the TRAILBLAZER and gantenerumab in the GRADUATE studies, demonstrating the capability to generalize beyond the dosing schedules (including intravenous and subcutaneous



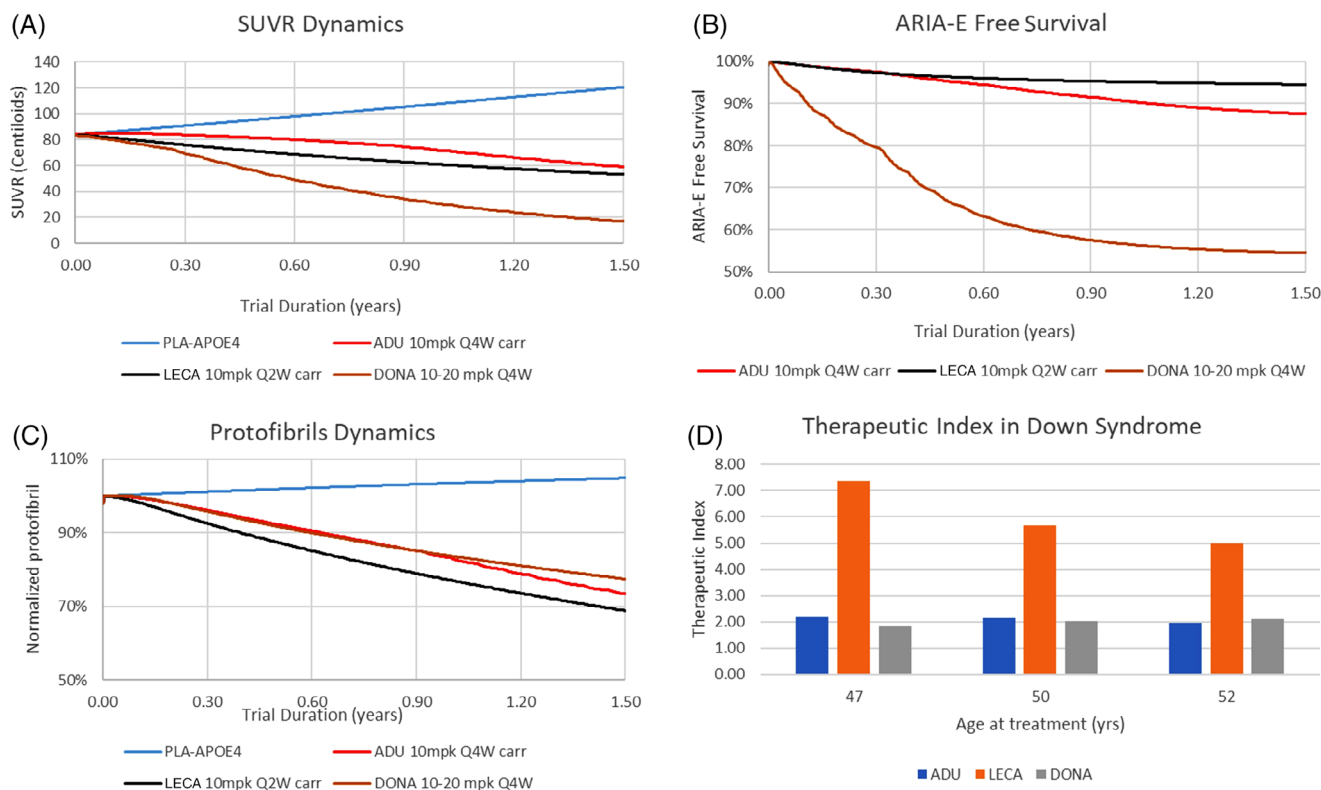


**FIGURE 6** Simulation of biomarkers in Down syndrome patients when treated at 47 years using the titration schedule for the Phase 3 studies in AD with 25% non-APOE4 and 75% APOE4+ carrier. (A) Central amyloid decrease is much greater for donanemab compared to aducanumab and lecanemab. (B) For APOE4+ patients, the same order is observed for ARIA-E side effects with donanemab a much greater liability. (C) Despite having a relatively modest central amyloid reduction, lecanemab has the greatest effect on protofibril clearance. (D) Lecanemab is superior with regard to the therapeutic index, defined as the ratio of normalized central amyloid decline divided by ARIA-liability. These outcomes are qualitatively similar for different trial start dates. AD, Alzheimer's disease; ADU, aducanumab; APOE4, apolipoprotein E  $\epsilon$ 4 allele; ARIA-E, amyloid-related imaging abnormality–edema; CL, centiloids; DONA, donanemab; LECA, lecanemab; mpk, mg/kg; PLA, placebo; SUVR, standardized uptake value ratio.

application) and pharmacology of the antibodies used for calibration. Therefore this model could in principle be expanded to also simulate the impact of novel amyloid therapies—many already in early clinical development—with different targets for instance focused solely on oligomers,<sup>24</sup> gamma-secretase modulators,<sup>25</sup> or with small molecules affecting the aggregation rate of A $\beta$  species.<sup>26,27</sup>

Based on the consensus that amyloid antibody therapy is best terminated after reaching amyloid negativity, we first simulated the time to reach this point for the three amyloid antibodies with different baseline amyloid levels. As expected, donanemab has the fastest clearance of central brain amyloid, while lecanemab and aducanumab have a slower, but very similar efficacy. We also demonstrated the slower A $\beta$  clearance by gantenerumab with a dosing schedule from the GRADUATE Phase 3 studies, as determined by PET imaging.<sup>8</sup>

While it has been extensively documented that CSF A $\beta$ 42 levels correlate inversely with central amyloid load in natural history progression, the impact of brain amyloid clearance by antibodies on changes in peripheral fluid A $\beta$  levels is more complex. Indeed, experimental observations after 18 months of treatment suggest almost a doubling of the A $\beta$ 42 CSF levels after lecanemab,<sup>28</sup> compared to a much more modest increase with donanemab,<sup>29</sup> despite the greater

effect on amyloid clearance. Simulations with the QSP model suggest that the increase in fluid A $\beta$  biomarkers is likely dependent upon the pharmacology of the antibody and generate the hypothesis that this observation is driven by the differential affinity of the antibodies for the more proximal low-order oligomer A $\beta$  forms which are linked to monomer dynamics through primary nucleation. Preferential elimination of these low-order oligomers by lecanemab leads to the synthesis of A $\beta$  monomers becoming more dominant compared to the aggregation into higher order aggregates. This results in higher ISF monomer A $\beta$  levels, which ultimately reflects in a larger peak of the CSF A $\beta$ 42 levels and opens the possibility to use these fluid biomarkers to help identify the time at which the antibody has completely cleared the central amyloid load. The lecanemab-associated CSF A $\beta$ 42 increase can be readily detected and is much greater than for aducanumab and donanemab. Similarly, the plasma A $\beta$ 42/A $\beta$ 40 ratio demonstrates a greater increase for lecanemab, suggesting that the use of these fluid biomarkers is less appropriate for aducanumab and donanemab.

Once brain amyloid negativity has been reached, maintenance dosing can be initiated to keep the amyloid load below the threshold. It has to be noted that because the disease-associated microglia (DAM) phe-

notype has a finite lifetime (about 1 year), the phagocytotic capacity only very gradually declined to the non-stimulated situation, allowing plaques to be cleared further after the antibody is gone. This explains the slight acceleration of central amyloid increase at longer times after treatment halt.

The model suggests that after halting donanemab treatment at amyloid negativity, central amyloid recovers on average about 3.5 CL/year. Clinical studies of donanemab have suggested that after treatment halt, it takes 3.9 years for patients who became amyloid negative to recover to a threshold of 25 CL,<sup>30</sup> well within the range of our predictions. In contrast, central amyloid recovers about 4.5 CL/year after lecanemab treatment. This is likely due to the differential pharmacology, with lecanemab affecting more upstream forms of A $\beta$  as compared to donanemab that very selectively binds to amyloid plaques, which contribute most to the central SUVR amyloid signal. In line with this hypothesis, the virtual patient trial suggests a faster slope of central amyloid rebound for those patients that end at higher central amyloid outcomes after treatment. The precise balance between primary nucleation and secondary nucleation (using amyloid plaques to enhance aggregation) defines the subsequent trajectory of the A $\beta$  species and therefore the imaging central amyloid readout, as outlined in the Methods section. As a note of caution, keeping amyloid negativity below threshold does not unequivocally lead to cognitive stabilization, as other pathological processes such as tau and neuroinflammation are not affected to the same degree.

Along the same lines, the virtual patient trial suggests that at 18 months, 78%, 72%, and 57% respectively of patients in the donanemab, lecanemab, and aducanumab trial were amyloid-negative. This is in accordance with reported clinical data of 71% for donanemab,<sup>31</sup> >75% for lecanemab,<sup>28,32</sup> and 48% for the EMERGE aducanumab trial.<sup>33</sup> It must be noted, however that the baseline central amyloid for lecanemab's CLARITY trial was much lower (77 CL) than for the other antibodies. The patients who did not reach amyloid negativity likely needed longer treatment and therefore were less responsive to that particular antibody treatment. A possible extension from this virtual patient study would be to identify the specific biological processes that would drive the therapeutic index for each of the antibodies, therefore possibly allowing for selection of the best antibody at the individual patient level.

Our QSP modeling platform suggests an optimal titration schedule for restarting therapy after an ARIA-E-related treatment interruption. In such a case, the additional delay to reach amyloid negativity (not including the 12-week treatment halt) ranges from 3 to 7 months which is relatively small compared to the slow progression of the disease. Interestingly, these simulations would predict that even in the absence of ARIA-E, a drug holiday during the first months of treatment can significantly reduce the accumulated liability of ARIA-E (maximally 12%, 8%, and 16% for donanemab, lecanemab, and aducanumab, respectively) with a relative minor effect on the decrease in amyloid load. These interesting predictions need to be confirmed in a clinical trial; however, the current model allows for the simulation of various titration and drug holiday schedules to significantly improve the initial planning of clinical trials or treatment guidelines.

DS patients will likely benefit greatly from these amyloid antibody therapies<sup>34,35</sup> and have been considered only rarely for clinical trials. The availability of amyloid antibodies opens the possibility to finally start treating these patients at an earlier age. We implemented a "DS" phenotype by increasing APP synthesis by 50%, based on the genetic signature of trisomy 21<sup>17</sup> and the observation that only subjects with triple APP gene evolved to the clinical phenotype. We acknowledge that this assumption does not take into account the large variability, the presence of mosaicism in the brain of DS patients, and the effect of aging on the amyloid clearance mechanisms.<sup>36,37</sup> While this can be addressed in further studies using a virtual patient approach, we wanted to contribute to the discussion of testing amyloid antibody therapies in DS patients.

Applying the QSP model to DS patients suggests that the same rank order will be preserved, that is, donanemab (dona) > lecanemab (leca)  $\geq$  aducanumab (adu) for reduction of central amyloid, while ARIA-E liability is much greater for dona > adu > leca. The therapeutic index is relatively independent of time of treatment and shows the same rank order as in AD patients, that is, leca > adu = dona. Many of the same readouts in terms of achieving amyloid negativity, the use of peripheral fluid biomarkers for detecting amyloid negativity, maintenance dosing after reaching amyloid negativity, and the impact of titration after an ARIA-E incident can be applied in this patient population using this QSP model.

The platform has a number of limitations. While the parameters were constrained and calibrated using data from observational natural history and interventional amyloid antibody studies using the reported patient populations, the results might not be generalizable to other situations, like different ages and baseline amyloid loads or different biology that drives the dynamics of A $\beta$  aggregation. However, the fact that we were able to reproduce the biomarker changes of donanemab TRAILBLAZER and gantenerumab GRADUATE studies suggest that the model captures well the underlying biological processes of A $\beta$  aggregation. Furthermore, group average outcomes of the virtual patient trial where the biological parameters were sampled from a Gaussian distribution recapitulated the clinical differentiation between the three antibodies.

A major concern is the determination of the affinities of the antibodies for the different A $\beta$  subspecies.<sup>38</sup> They are not always easy to measure accurately and are clear drivers of the biomarker responses. Here we applied the binding affinities as summarized in the QSP paper.<sup>6</sup>

Another possible concern is the increase of the BBB leakiness, either associated with age or with the APOE genotype,<sup>36,37</sup> that is currently not implemented in the model. This might overpredict the proposed readouts in DS patients and can affect the outcome of the virtual patient trial. An updated version of the model will take this important parameter into account.

Because it has been suggested that protofibrils were an important A $\beta$  species driving neurotoxicity,<sup>10</sup> we compared the reduction in free protofibrils with the different antibodies at the time of reaching amyloid negativity. Lecanemab is by far the most efficient drug, which is not unexpected given its selectivity for this type of A $\beta$  fibrils. However,

this outcome needs to be interpreted cautiously, as the time to reach amyloid negativity can substantially differ between the different drugs. For instance, compared to donanemab, lecanemab needs a longer time to achieve amyloid negativity, and therefore can clear protofibril levels more efficiently.

A more appropriate fluid biomarker would be plasma p-tau217; however the relationship between changes in amyloid load following treatment and changes in this biomarker are currently beyond the scope of this mechanistic model and will be addressed in further work.

Finally, the biggest challenge is the link to cognitive readouts where donanemab and lecanemab show a robust effect slightly greater than aducanumab. Studying the antibody-specific dynamics of the different A $\beta$  species and relating them to clinical outcome could illuminate the biological processes that drive cognitive outcome. It has to be noted that recently a comprehensive semi-mechanistic model<sup>39</sup> was published linking amyloid changes over tau pathways to clinical outcomes. It might be of substantial interest to combine this model with the more detailed amyloid aggregation model presented here to support further therapeutic developments.

Future work is focused on an extensive sensitivity analysis of the QSP platform using the virtual patient approach. This would allow identifying the biological processes that would (1) specifically drive biomarker response for each of the three antibodies, (2) be associated with higher ARIA-E liability, and (3) drive fast re-aggregation after reaching amyloid negativity. If we can find any biomarkers (clinical or genetic) associated with these biological processes, treatment could be more personalized.

QSP has been traditionally used in late drug discovery and early clinical development because it is based on biology and is optimal for data-poor situations, although recently QSP has proven to be useful in late clinical development. We believe that this model, which is well calibrated with a large amount of clinical data from the last 20 years, would be very helpful in supporting clinical trial design of future amyloid therapeutics and in new amyloid pathology-driven indications. To our knowledge, this is also the first example where QSP has been applied to address challenges in clinical practice of AD treatment.

In summary, this report demonstrates that the QSP amyloid platform presented here could be applied to many different situations, because it is firmly based on the biophysical principles of protein aggregation. As such it can lay the groundwork for applying this type of mechanistic pharmacological modeling to real-world clinical situations.

## ACKNOWLEDGMENTS

H.G., M.W., S.B., R.R. and P.vdG. are or were employees of Certara at the time of the study. We appreciate the critical reading and feedback of Dr. Shaina Short.

## CONFLICT OF INTEREST STATEMENT

The authors do not have any conflicts of interest. Author disclosures are available in the [Supporting Information](#).

## ORCID

Hugo Geerts  <https://orcid.org/0000-0002-9736-1800>

## REFERENCES

1. Angioni D, Hansson O, Bateman RJ, et al. Can we use blood biomarkers as entry criteria and for monitoring drug treatment effects in clinical trials? A report from the EU/US CTAD task force. *J Prev Alzheimers Dis.* 2023;10:418-425.
2. Alzheimer's association launches ALZ-NET: a long-term data collection and sharing network for new treatments. *Alzheimers Dement.* 2022;18:1694-1695.
3. Cummings J, Apostolova L, Rabinovici GD, et al. Lecanemab: appropriate use recommendations. *J Prev Alzheimers Dis.* 2023;10:362-377.
4. Cummings J, Rabinovici GD, Atri A, et al. Aducanumab: appropriate use recommendations update. *J Prev Alzheimers Dis.* 2022;9:221-230.
5. Howe MD, Britton KJ, Joyce HE, et al. Initial experiences with amyloid-related imaging abnormalities in patients receiving Aducanumab following accelerated approval. *J Prev Alzheimers Dis.* 2023;10:765-770.
6. Geerts H, Walker M, Rose R, et al. A combined physiologically-based pharmacokinetic and quantitative systems pharmacology model for modeling amyloid aggregation in Alzheimer's disease. *CPT Pharmacometrics Syst Pharmacol.* 2023;12(4):444-461.
7. Mintun MA, Lo AC, Duggan Evans C, et al. Donanemab in early Alzheimer's disease. *New England J Med.* 2021;384:1691-1704.
8. Bateman RJ, Smith J, Donohue MC, et al. Two phase 3 trials of gantenerumab in early Alzheimer's disease. *N Engl J Med.* 2023;389:1862-1876.
9. Hanseeuw BJ, Malotau V, Dricot L, et al. Defining a Centiloid scale threshold predicting long-term progression to dementia in patients attending the memory clinic: an [(18)F] flutemetamol amyloid PET study. *Eur J Nucl Med Mol Imaging.* 2021;48:302-310.
10. Chen ZL, Singh PK, Calvano M, Norris EH, Strickland S. A possible mechanism for the enhanced toxicity of beta-amyloid protofibrils in Alzheimer's disease. *Proc Nat Acad Sci USA.* 2023;120:e2309389120.
11. Chang HY, Wu S, Meno-Tetang G, Shah DK. A translational platform PBPK model for antibody disposition in the brain. *J Pharmacokinetic Pharmacodyn.* 2019;46:319-338.
12. Sehlin D, Englund H, Simu B, et al. Large aggregates are the major soluble Abeta species in AD brain fractionated with density gradient ultracentrifugation. *PLoS One.* 2012;7:e32014.
13. Lin YT, Seo J, Gao F, et al. APOE4 causes widespread molecular and cellular alterations associated with Alzheimer's disease phenotypes in human iPSC-derived brain cell types. *Neuron.* 2018;98:1141-1154 e7.
14. Navitsky M, Joshi AD, Kennedy I, et al. Standardization of amyloid quantitation with florbetapir standardized uptake value ratios to the Centiloid scale. *Alzheimers Dement.* 2018;14:1565-1571.
15. Kuhlmann J, Andreasson U, Pannee J, et al. CSF Abeta(1-42)—an excellent but complicated Alzheimer's biomarker—a route to standardisation. *Clin Chim Acta.* 2017;467:27-33.
16. Salvado G, Molinuevo JL, Brugulat-Serrat A, et al. Centiloid cut-off values for optimal agreement between PET and CSF core AD biomarkers. *Alzheimers Res Ther.* 2019;11:27.
17. Head E, Helman AM, Powell D, Schmitt FA. Down syndrome, beta-amyloid and neuroimaging. *Free Radical Biol Med.* 2018;114:102-109.
18. Lowe SL, Duggan Evans C, Shcherbinin S, et al. Donanemab (LY3002813) Phase 1b study in Alzheimer's disease: rapid and sustained reduction of brain amyloid measured by Florbetapir F18 imaging. *J Prev Alzheimers Dis.* 2021;8:414-424.
19. Lowe SL, Willis BA, Hawdon A, et al. Donanemab (LY3002813) dose-escalation study in Alzheimer's disease. *Alzheimer Dementia.* 2021;7:e12112.
20. Demattos RB, Lu J, Tang Y, et al. A plaque-specific antibody clears existing beta-amyloid plaques in Alzheimer's disease mice. *Neuron.* 2012;76:908-920.
21. Aldea R, Grimm HP, Gieschke R, et al. In silico exploration of amyloid-related imaging abnormalities in the gantenerumab open-label extension trials using a semi-mechanistic model. *Alzheimer Dementia.* 2022;8:e12306.

22. Lord A, Gumucio A, Englund H, et al. An amyloid-beta protofibril-selective antibody prevents amyloid formation in a mouse model of Alzheimer's disease. *Neurobiol Dis.* 2009;36:425-434.
23. Sollvander S, Nikitidou E, Gallasch L, et al. The Abeta protofibril selective antibody mAb158 prevents accumulation of Abeta in astrocytes and rescues neurons from Abeta-induced cell death. *J Neuroinflam.* 2018;15:98.
24. Krafft GA, Jerecic J, Siemers E, Cline EN. ACU193: an immunotherapeutic poised to test the amyloid beta oligomer hypothesis of Alzheimer's disease. *Front Neurosci.* 2022;16:848215.
25. Rynearson KD, Ponnusamy M, Prikhodko O, et al. Preclinical validation of a potent gamma-secretase modulator for Alzheimer's disease prevention. *J Exp Med.* 2021;218.
26. Re F, Airoldi C, Zona C, et al. Beta amyloid aggregation inhibitors: small molecules as candidate drugs for therapy of Alzheimer's disease. *Curr Med Chem.* 2010;17:2990-3006.
27. Arar S, Haque MA, Kayed R. Protein aggregation and neurodegenerative disease: structural outlook for the novel therapeutics. *Proteins.* 2023.
28. McDade E, Cummings JL, Dhadda S, et al. Lecanemab in patients with early Alzheimer's disease: detailed results on biomarker, cognitive, and clinical effects from the randomized and open-label extension of the phase 2 proof-of-concept study. *Alz Res Therapy.* 2022;14:191.
29. Pontecorvo MJ, Lu M, Burnham SC, et al. Association of donanemab treatment with exploratory plasma biomarkers in early symptomatic alzheimer disease: a secondary analysis of the TRAILBLAZER-ALZ randomized clinical trial. *JAMA Neurology.* 2022;79:1250-1259.
30. Shcherbinin S, Evans CD, Lu M, et al. Association of amyloid reduction after donanemab treatment with tau pathology and clinical outcomes: the TRAILBLAZER-ALZ randomized clinical trial. *JAMA Neurol.* 2022;79:1015-1024.
31. Sims JR, Zimmer JA, Evans CD, et al. Donanemab in early symptomatic Alzheimer disease: the TRAILBLAZER-ALZ 2 randomized clinical trial. *JAMA.* 2023;330:512-527.
32. van Dyck CH, Swanson CJ, Aisen P, et al. Lecanemab in early Alzheimer's disease. *New England J Med.* 2023;388:9-21.
33. Budd Haeberlein S, Aisen PS, Barkhof F, et al. Two randomized phase 3 studies of aducanumab in early Alzheimer's disease. *J Prevention Alzheimer Disease.* 2022;9:197-210.
34. Rafii MS. Alzheimer's disease in Down syndrome: progress in the design and conduct of drug prevention trials. *CNS Drugs.* 2020;34:785-794.
35. Strydom A, Coppus A, Blesa R, et al. Alzheimer's disease in Down syndrome: an overlooked population for prevention trials. *Alzheimers Dement.* 2018;4:703-713.
36. Montagne A, Nation DA, Sagare AP, et al. APOE4 leads to blood-brain barrier dysfunction predicting cognitive decline. *Nature.* 2020;581:71-76.
37. Montagne A, Toga AW, Zlokovic BV. Blood-brain barrier permeability and gadolinium: benefits and potential pitfalls in research. *JAMA Neurol.* 2016;73:13-14.
38. Zhang T, Nagel-Steger L, Willbold D. Solution-based determination of dissociation constants for the binding of Abeta42 to antibodies. *ChemistryOpen.* 2019;8:989-994.
39. Mazer NA, Hofmann C, Lott D, et al. Development of a quantitative semi-mechanistic model of Alzheimer's disease based on the amyloid/tau/neurodegeneration framework (the Q-ATN model). *Alzheimers Dement.* 2023;19:2287-2297.

#### SUPPORTING INFORMATION

Additional supporting information can be found online in the Supporting Information section at the end of this article.

**How to cite this article:** Geerts H, Bergeler S, Walker M, Rose RH, van der Graaf PH. Quantitative systems pharmacology-based exploration of relevant anti-amyloid therapy challenges in clinical practice. *Alzheimer's Dement.* 2024;10:e12474. <https://doi.org/10.1002/trc2.12474>